THE LIMITED APPLICABILITY OF WIENER FILTERING TO ECG SIGNALS DISTURBED BY THE MHD EFFECT

J.W. Krug[1], *G.D. Clifford*[2], *G.H. Rose*[1], *J. Oster*[2]

[1]Chair for Healthcare Telematics and Medical Engineering, University of Magdeburg, Germany
[2]Department of Engineering Science, University of Oxford, Oxford, UK

ABSTRACT

The diagnostic information of an electrocardiogram (ECG) is essential to ensure patient safety in interventional procedures or medical diagnostics, e.g. during cardiac stress testing. When performing these interventional or diagnostic procedures inside an magnetic resonance imaging (MRI) environment, the ECG is directly and indirectly distorted by the several magnetic fields. While it is still possible to detect the QRS complex which is necessary for gating cardiac image sequences, a diagnostic interpretation of the ECG itself is not possible.

In an attempt to remove the distortion due to the magnetohydrodynamic (MHD) effect, a model of the undistorted ECG was constructed outside the scanner using a Wiener filter. The filter was then applied in a forward sense to the ECG recorded inside an MR scanner. Clinical features, such as the ST level and QT interval were measured before and after filtering and compared to the nominal values taken prior to MRI scanning.

Errors in ST level estimation were sometimes found to be greater than 0.1mV, indicating that diagnostic accuracy cannot always be maintained. However, the results for QT interval analysis are sometimes within acceptable tolerances (10 ms-30 ms). This work therefore provides a standard benchmark for other approaches to beat.

Index Terms— ECG, Magnetohydrodynamic Effect, MRI, Wiener Filter

1. INTRODUCTION

Magnetic resonance imaging (MRI) plays an important role in medical examinations and interventions. The examinations include - besides anatomic imaging - functional diagnostics like cardiac stress testings [1], [2]. Minimal invasive interventions like biopsies or electrophysiological studies are performed as well in the MR scanner due to certain advantages of MR images compared to X-ray/CT/Ultrasonic images [3], [4]. ECG monitoring is recommended for interventions that require anesthesia or sedation [5]. Besides patient monitoring, the acquisition of an ECG is necessary for gating purposes during cardiac MRI.

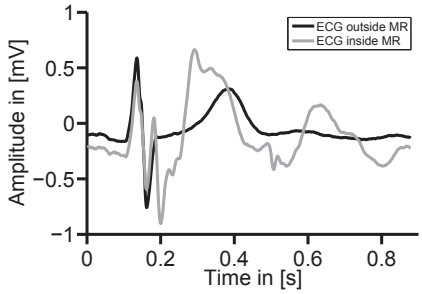

Fig. 1. Lead I of an ECG signal measured outside (black) and inside (grey) an MR scanner while MR imaging is turned off.

Both, monitoring and gating, are disturbed by the hostile environment of the MR scanner. The presence of three different types of magnetic fields within an MR scanner leads to these difficulties. *High frequency fields* - typically above 42 MHz and with magnetic flux densities in the range of a few μT - impose a safety risk to both, patient and ECG hardware due to coupling and resonance effects. *Gradient magnetic fields* with frequencies mainly below 1 kHz and in the range of 100 $^{\mathrm{mT}}/_{\mathrm{m}}$ lead to severe distortions of the ECG signal making it hard to detect the QRS complex which is of big importance in cardiac gating. Much research effort has been made to reduce the gradient induced signals in the ECG [6].

The MR scanner's *static magnetic field* which is typically in the range of 1 T to 3 T in clinical scanners and up to 9.4 T in research scanners induces a disturbing signal caused by the magnetohydrodynamic (MHD) effect [7, 8]. The MHD effect is caused by the flow of blood perpendicular to the static magnetic field. An example for an ECG recorded in a 1.5 T MR scanner is shown in Fig. 1. Few methods have been applied to reduce the MHD effect in the ECG [9].

In this work we aimed to construct a simple filtering method to provide a baseline value for more complex methods to beat. Metrics for success were defined in terms of relevant clinical parameters.

2. THEORY

2.1. MHD effect overview

Blood plasma, which makes up about 60 % of the total blood volume contains approximatly 10 % solutes such as Na^+, Cl^- or HCO_3^- ions. These ions are moving inside the vessels where they experience a force due to the presence of the external magnetic field - namely the MR scanner's magnetic $\vec{B}_0$ field. This force is known as Lorentz force $\vec{F}$:

$$\vec{F} \propto (\vec{v} \times \vec{B}_0) \tag{1}$$

and depends on the magnitude and orientation of the blood flow velocity $\vec{v}$ with respect to the magnetic field, $\vec{B}_0$. This force causes the ions to move perpendicular to the direction of the blood flow and perpendicular to $\vec{B}_0$. The ions accumulate near the vessel's wall leading to a potential difference across the vessel that may be expressed as:

$$V \propto \int_0^l \vec{v} \times \vec{B}_0 \, d\vec{l} \tag{2}$$

where l is the diameter of the vessel. This is the so called MHD effect. Besides these basic assumptions, additional parameters as the density, conductivity and viscosity of blood, the Hartmann number or the aortic blood pressure have to be considered to estimate the induced voltage across the vessel [10]. Furthermore, additional transfer functions are used to estimate the body surface potentials [11].

2.2. Properties of the ECG and MHD signals

The MHD signal heavily depends on the mechanical activation of the myocardium and is thereby highly correlated to the ECG signal. The electrical activation of the myocardium results in a mechanical contraction leading to the ejection of blood into the ascending aorta and all subsequent blood vessels. This flow of blood is affected by the MR scanner's static magnetic field which finally gives rise to the MHD effect as described in section 2.1. The MHD effect influences the ECG mainly in the ST segment and the T wave since this corresponds to the systolic phase of the heart cycle.

Figure 2 shows the time-frequency energy distributions (TFED) for the ECG and MHD signals. The TFEDs were estimated using a Smoothed Pseudo Wigner-Ville Distribution with window lengths h = 140 ms and g = 70 ms. The MHD signal was calculated by subtracting an averaged ECG signal recorded outside the MR scanner from an averaged ECG signal recorded inside the MR scanner. Both averaged signals were calculated over ten consecutive heart beats. Note that there is a large overlap in time and frequency between the cardiac and MHD induced signals, particularly around 0-10 Hz, and 0.1-0.3 s after the QRS complex (located at around 0.15 s). Note that the magnitude of the MHD exceeds those of the ECG signal, and that this region is in the time-frequency plane corresponding to the T wave and ST segment. Therefore, standard low-pass or high-pass filtering (even using time-frequency methods) is unlikely to be useful.

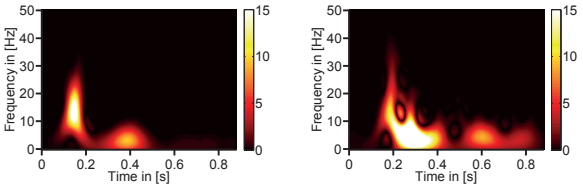

(a) ECG signal, Lead I (b) MHD signal, Lead I

Fig. 2. Comparison of the time-frequency energy distributions of the ECG and the MHD signal in $^{mV^2}/_{Hz}$. The time scale is the same as in Figs. 1 and 3 with the R peak located at about 150 ms.

For the measurements in the 1.5 T MR scanner, the amplitude of the MHD signal is of the order of the amplitude of the R-peak within the limb leads. The MHD effect is more severe for higher field strength as described by Eq. 2 or for MR scanners with a vertical orientation of the magnetic field as demonstrated in [8].

2.3. Importance of clinical features

The morphology of the ST segment and the duration of the QT interval are important for the clinical diagnosis of cardiac malfunctions like an acute myocardial ischemia or ventricular arrhythmias. An *elevation* of the ST segment in two contiguous leads is considered to be significant if it exceeds 0.2 mV in lead V_1, V_2 or V_3 and 0.1 mV in other leads [12]. The duration of the QT interval is the time difference between the onset of the QRS complex and the offset of the T wave. It is characterized as pathological when it exceeds 430 ms.

2.4. Causal Wiener Filter

The Wiener filter is the optimal filter in the sense of minimizing the mean squared error (MSE) between an estimated filter output $\widehat{y}$ and the desired filter output signal y. The error is defined as $e = y - \widehat{y}$ with the MSE defined as:

$$E[e^2] = E\left[(y - \widehat{y})^2\right] = E\left[(y - \mathbf{w}^T\mathbf{x})^2\right] \tag{3}$$

where $E[\cdot]$ is the expectation operator, $\mathbf{w}$ the Wiener filter coefficient vector and $\mathbf{x}$ the input signal vector to the Wiener filter. The minimization of the MSE in Eq. 3 leads to the following equation to estimate the Wiener filter coefficient vector:

$$\mathbf{w} = \mathbf{R}_{xx}^{-1}\mathbf{r}_{xy} \tag{4}$$

where $\mathbf{R}_{xx}$ is the autocorrelation matrix of the filter input signal $\mathbf{x}$ and $\mathbf{r}_{xy}$ the cross-correlation vector between $\mathbf{x}$ and the desired filter output signal vector $\mathbf{y}$.

3. MATERIAL AND METHODS

3.1. ECG data acquisition and preprocessing steps

The ECG signals used in this work were recorded in a 1.5 T MR scanner (Siemens Magnetom Vision) at the Magdeburg University Hospital. Measurements were made on one healthy male volunteer aged 28. The ECGs were recorded outside and inside the MR scanner during breath hold in supine position, with each measurement being 20 s long.

A standard 12-lead Holter ECG (*CardioMem CM3000-12, GETEMED, Germany*) with a sampling rate of 1024 Hz, a resolution of 12 Bit, an input voltage range of ± 6 mV and an analogue bandwidth ranging from 0.05 Hz to 100 Hz was used for recording the ECGs. In order to operate from the outside of the MR scanner, the lead cables were extended. Standard MR-safe ECG Electrodes were used and MR imaging was switched off during all measurements to avoid additional disturbing signals.

The ECG signals are manually split into segments of 900 ms length, with the R peaks being aligned at 150 ms, so that each segment starts approximatively at the onset of the P wave. Each segment has been centred, meaning its mean is equal to zero.

3.2. Estimation of the Wiener filter coefficients

Given the assumption that the ECG signal has different dynamics for each different phase and in order to focus on the Wiener filter's ability to work properly on the ST segment and the T wave of the ECG, a segment of 500 ms length starting 20 ms after the R peak was used for the estimation of the Wiener filter coefficients (Fig. 3). This segment contains the S peak, the J point, the ST segment and the whole T wave including a short subsequent section. By keeping the mathematical notation introduced in section 2.4, **x** is the ECG signal recorded inside the MR scanner which is disturbed by the MHD effect and **y** is the ECG signal from the same patient recorded outside the MR scanner. Ten segments of the disturbed signal **x** are used to estimate the Wiener filter coefficients in Eq. 4. The desired output signal **y** is a clean ECG which is estimated by taking the mean of ten consecutive heart beats which have the same dominant morphology. Using **x** and **y**, 200 Wiener filter coefficients **w** are estimated for the segment described above. The number of coefficients is a compromise between the frequential complexity of the relation between the MHD and the ECG signal and the non-overfitting of the learning problem.

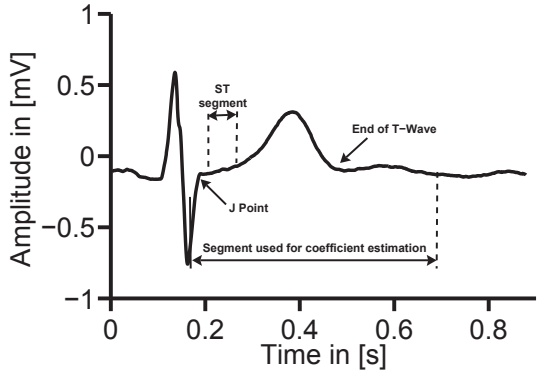

Fig. 3. Regions of interest for Wiener filtering and the subsequent analysis within one segment of the ECG .

3.3. QT interval, amplitude error and SNR estimation

The *QT interval* estimation is made difficult during MRI, especially since the T wave offset lies in the MHD noise. A medical ECG expert annotated the end of the T wave in the desired ECG signal **y** recorded outside the MR scanner and in the Wiener filtered ECG signals $\widehat{\mathbf{y}}$. The end of the T wave was defined at the intersection between the tangent in the steepest slope of the T wave with the isoelectric line [13]. The isoelectric level was estimated from the TP segment.

The *amplitude error* in the ST segment and in the complete segment of 500 ms length described in Section 3.2 is measured as the mean absolute difference between the desired signal **y** and the filter output signal $\widehat{\mathbf{y}}$. For the ST segment, the error is calculated for a section of 20 ms length starting from *J point* + 80 ms.

The *Signal-to-Noise-Ratio (SNR)* gives an estimate of the ratio between the desired output signal **y** and the noise contained in it. The SNR is estimated for the disturbed ECG signal **x** before and for the estimated signal $\widehat{\mathbf{y}}$ after filtering using the following equation:

$$\mathrm{SNR} = 10 \cdot \log \left(\frac{\sigma_S^2}{\sigma_N^2} \right) \mathrm{dB} \tag{5}$$

where σ_S^2 is the variance of the desired signal y. σ_N^2 is the variance of the noise which is defined as the residual between the desired signal y and either the filter input signal x or the filter output signal $\widehat{y}$ in order to estimate the SNR before and after filtering, respectively. The SNR is estimated for *a)* only the ST segment and *b)* for the complete segment of 500 ms length.

4. RESULTS

4.1. Visual evaluation of the results

The Wiener filter gave highly varying results from lead to lead. As an example, a selection of filtered ECG leads is shown in Fig. 4. For this example, the error within the ST segment for leads I and II is larger than in lead V1. These clinical important errors in the ST segment and the T wave are analysed in the following sections.

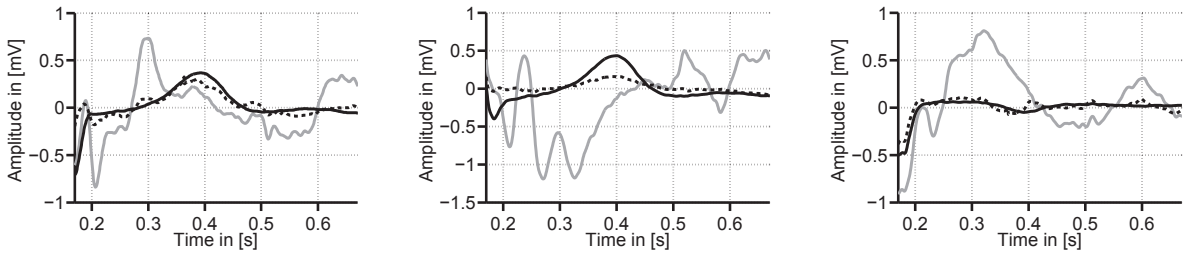

(a) Lead I (b) Lead II (c) Lead V1

Fig. 4. Input signal (gray), desired signal (black) and Wiener filter output signal (dashed) in different ECG leads.

4.2. Annotation of the T wave's end

The T wave could be annotated in almost all of the leads of the filtered signal $\widehat{\mathbf{y}}$. Lead V1 gave the worst results since the T wave amplitude is minimal in this lead as shown in Fig. 4(c). The best results were obtained in leads II, III, V2, V3 and V6 whereas it is recommended to measure the QT segment in leads II and V5 or V6 [14]. The error in the manual annotation of the T wave's end position in the Wiener filtered signals was between 20-30 ms. This is less precise than results achieved by manual annotation of undistorted ECG signals [15]. The main challenge was to estimate the isoelectric level in the filtered ECG signal $\widehat{\mathbf{y}}$ in order to annotate the T wave's end.

4.3. Amplitude error measurements in the ST segment

To investigate the Wiener filters ability to track a desired signal, the error between the desired ECG signal $\mathbf{y}$ and the output of the Wiener filter $\widehat{\mathbf{y}}$ has been estimated. The filter was successively applied to ten of the ECG segments described in Section 3.2. The minimal and maximal errors in each channel of the ten filtered heart cycles are given in Table 1. The maximum error in the ST-segment is above or close to 0.1 mV in leads I and II which could lead to a false detection of ischemia.

4.4. SNR estimation

Table 2 shows the SNR for all 12 ECG leads. The SNR within the ST segment is increased by approximately 40 dB after filtering. The SNR is lower on the ST segment than on the whole 500 ms segment, highlighting the complexity of estimating the ST segment elevation.

5. SUMMARY AND CONCLUSION

The Wiener filter was applied to ECG signals corrupted by the MHD effect. It was applied to a segment of 500 ms length containing the S peak, the ST segment, the T wave and a short subsequent period.

The amplitude errors measured within the ST segment are of high importance since part of the leads show maximum errors around 0.1 mV. These errors can lead to a false diagnosis of ischemia.

A clinical expert estimated the end of the T waves in the clean ECGs recorded outside the MR scanner and in the Wiener filtered signals. The estimation error was between 20-30 ms which is less accurate than the manual annotation of clean ECG signals but in the range of automated analysis [16].

Although the SNR increased within the ST segment as well as in the whole 500 ms segment after filtering, a high level of noise due to oscillations in the ST segment induced by the filtering process remains. However, for the clinical analysis of the ST segment and the estimation of the T wave's end, the SNR is not relevant.

It has to be taken into account that the whole filter process can be regarded as an *ideal situation* since the underlying ECG signal $\mathbf{y}$ as well as the MHD effect were only subject to small changes. However, as shown in Fig. 4 and Table 1, the filter output signal $\widehat{\mathbf{y}}$ shows clinically significant deviations from the desired signal $\mathbf{y}$. For the *non-ideal situation*

Table 1. Amplitude error after Wiener filtering within the ST segment.

Lead	Min in [mV]	Max in [mV]
I	0.045	0.119
II	0.046	0.083
III	0.027	0.055
aVR	0.005	0.022
aVL	0.023	0.046
aVF	0.018	0.028
V1	0.012	0.055
V2	0.013	0.097
V3	0.055	0.122
V4	0.018	0.035
V5	0.027	0.053
V6	0.013	0.034

Table 2. SNR mean and standard deviations (in dB) in the ST segment and the 500 ms segment before and after filtering.

	ST segment		ST segment & T wave	
Lead	Before	After	Before	After
I	-52 ± 5	-13 ± 8	-15 ± 2	8 ± 2
II	-74 ± 4	2 ± 6	-15 ± 5	6 ± 3
III	-103 ± 2	-53 ± 5	-36 ± 3	5 ± 1
aVR	-58 ± 6	6 ± 13	-9 ± 4	4 ± 2
aVL	-93 ± 2	-52 ± 3	-29 ± 1	7 ± 1
aVF	-85 ± 3	-23 ± 7	-26 ± 4	10 ± 3
V1	-82 ± 2	-33 ± 11	-22 ± 2	15 ± 2
V2	-38 ± 4	-4 ± 11	-6 ± 1	24 ± 1
V3	-25 ± 4	5 ± 11	-7 ± 1	14 ± 1
V4	-47 ± 3	-10 ± 5	-8 ± 2	9 ± 1
V5	-52 ± 3	-12 ± 3	-11 ± 2	13 ± 2
V6	-61 ± 4	-18 ± 5	-17 ± 3	17 ± 4

where the ECG and MHD signals are changing, e.g. due the breathing, changes in heart rate, cardiac output and rhythm or pathological disorders, it is expected that the performance of the Wiener filter will decrease. To confirm this hypothesis, more subjects and pathological patients or simulations of time-varying ECG waveforms need to be included.

In conclusion, the detection of the T wave's end gave acceptable results, which may be improved by enhancing the preservation of the ECG's isoelectric level after the filtering process. This needs to be confirmed on a larger patient database. Nevertheless, the results are not promising for measurements of ST segment, although the filter was applied in an ideal situation. This enlightens the limited applicability of Wiener filtering for this problem.

6. ACKNOWLEDGEMENT

Johannes Krug is funded by the Federal Ministry of Education and Research (BMBF, Germany) in context of the Innoprofile project 'INKA' (03IP710). Julien Oster is a Newton international fellow (round 2010 from the Royal Academy of Engineering). The ECG recording hardware was kindly provided by GETEMED AG, Germany.

7. REFERENCES

[1] M. Jekic, E. Foster, M. Ballinger, S. Raman, and O. Simonetti, "Cardiac function and myocardial perfusion immediately following maximal treadmill exercise inside the MRI room," *J Cardiovasc Magn Reson*, vol. 10, no. 3, 2008.

[2] J. Jeneson, J. Schmitz, P. Hilbers, and K. Nicolay, "An MR-Compatible Bicycle Ergometer for In-Magnet Whole-Body Human Exercise Testing," *Magnet Reson Med*, vol. 63, no. 1, pp. 257–261, 2010.

[3] F. Fischbach, J. Bunke, M. Thormann, G. Gaffke, K. Jungnickel, J. Smink, and J. Ricke, "MR-guided freehand biopsy of liver lesions with fast continuous imaging using a 1.0-T open MRI scanner: experience in 50 patients," *Cardiovasc Intervent Radiol*, vol. 34, no. 1, pp. 188–192, 2011.

[4] M. Gutberlet, M. Grothoff, C. Eitel, C. Lücke, P. Sommer, C. Piorkowski, and G. Hindricks, "First clinical experience in man with the IMRICOR-MR-EP system: Electrophysiology study guided by real-time MRI," *J Cardiovasc Magn Reson*, vol. 14, pp. 1–2, 2012.

[5] American Society of Anesthesiologists, "Practice Advisory on Anesthetic Care for Magnetic Resonance Imaging," *Anesthesiology*, vol. 110, no. 3, pp. 459–79, 2009.

[6] J. Oster, O. Pietquin, M. Kraemer, and J. Felblinger, "Bayesian framework for artifact reduction on ECG in MRI," in *Proc IEEE ICASSP*, 2010, pp. 489–492.

[7] G. Nijm, S. Swiryn, A. Larson, and A. Sahakian, "Characterization of the Magnetohydrodynamic Effect as a Signal from the Surface Electrocardiogram during Cardiac Magnetic Resonance Imaging," in *Proc IEEE Comput in Cardiol*, vol. 33, 2006, pp. 269–272.

[8] J. Krug and G. Rose, "Magnetohydrodynamic Distortions of the ECG in Different MR Scanner Configurations," in *Proc IEEE Comput in Cardiol*, vol. 38, 2011, pp. 769–772.

[9] Z. Tse, C. Dumoulin, G. Clifford, M. Jerosch-Herold, D. Kacher, R. Kwong, W. Stevenson, and E. Schmidt, "Improved R-wave detection for enhanced cardiac Gating using an MRI-compatible 12-lead ECG and multi-channel analysis," *J Cardiovasc Magn Reson*, vol. 13, pp. 1–3, 2011.

[10] Y. Kinouchi, H. Yamaguchi, and T. S. Tenforde, "Theoretical analysis of magnetic field interactions with aortic blood flow," *Bioelectromagnetics*, vol. 17, no. 1, pp. 21–32, 1996.

[11] V. Martin, A. Drochon, O. Fokapu, and J. Gerbeau, "MagnetoHemoDynamics Effect on Electrocardiograms," *FIMH*, pp. 325–332, 2011.

[12] E. Antman, J. Bassand, W. Klein, M. Ohman, J. Lopez Sendon, L. Rydén, M. Simoons, and M. Tendera, "Myocardial infarction redefined–a consensus document of The Joint European Society of Cardiology/American College of Cardiology committee for the redefinition of myocardial infarction," *JACC*, vol. 36, no. 3, p. 959, 2000.

[13] J. Johnson and M. Ackerman, "QTc: how long is too long?" *Br J Sports Med*, vol. 43, no. 9, pp. 657–662, 2009.

[14] I. Goldenberg, A. Moss, W. Zareba *et al.*, "QT interval: how to measure it and what is" normal"," *J Cardiovasc Electrophysiol*, vol. 17, no. 3, pp. 333–336, 2006.

[15] I. Christov, I. Dotsinsky, I. Simova, R. Prokopova, E. Trendafilova, S. Naydenov *et al.*, "Dataset of manually measured QT intervals in the electrocardiogram," *Biomed Eng Online*, vol. 5, no. 1, p. 31, 2006.

[16] G. Moody, H. Koch, and U. Steinhoff, "The PhysioNet/Computers in Cardiology Challenge 2006: QT Interval Measurement," in *Proc IEEE Comput in Cardiol*, vol. 33, 2006, pp. 313–316.